PCCP

PAPER

View Article Online
View Journal | View Issue

Cite this: *Phys. Chem. Chem. Phys.*, 2017, **19**, 24979

Superlinear amplification of the first hyperpolarizability of linear aggregates of DANS molecules†

Somananda Sanyal, [a] Cristina Sissa, [a] Francesca Terenziani, [a] Swapan K. Pati [b] and Anna Painelli *[a]

Received 13th July 2017,
Accepted 23rd August 2017

DOI: 10.1039/c7cp04732k

rsc.li/pccp

A bottom-up modelling strategy is adopted to discuss the linear and nonlinear optical spectra of a prototypical push–pull dye, 4-dimethylamino-4′-nitrostilbene (DANS), in different environments, from solutions to linear aggregates, fully accounting for the molecular polarity and polarizability. In particular, we demonstrate a large amplification of the first hyperpolarizability of linear aggregates with a superlinear dependence on the aggregate size. Results are discussed with reference to recent experiments for DANS molecules aligned inside single-wall carbon nanotubes, leading to a complete and internally consistent description of the observed spectral properties in terms of ~7 aligned molecules, reducing by an order of magnitude the size of the aggregate estimated in the hypothesis of linear amplification, as expected for non-interacting molecules. This has important implications for material design: it is possible to obtain a large amplification of the first hyperpolarizability by aligning just a few DANS molecules (or more generally, a few polar dyes showing normal solvatochromism) without the need to grow large ordered systems.

Introduction

Donor–acceptor (DA) or push–pull chromophores have been extensively investigated for their promising nonlinear optical (NLO) responses,[1] ensured by the presence of delocalized electrons and low-energy charge-transfer degrees of freedom.[2] The polar nature of DA dyes makes them extremely responsive to the polarity of the environment and their solvatochromism has been exploited for applications in polarity and electric field sensing.[3] Due to their asymmetric structures, DA dyes are the molecules of choice for second-order NLO responses (related to the first hyperpolarizability β) and have been quite extensively investigated in this respect.[1,4] A major issue hindering the successful development of second-order NLO materials based on DA dyes is the requirement that the asymmetry is maintained at the material (macroscopic) level. In fact, with few notable exceptions,[5] DA dyes organize themselves to maximize favourable electrostatic interactions forming centrosymmetric structures.[6] To overcome this problem, different strategies have been proposed. The most popular strategy consists of loading a polymeric matrix with DA dyes, then using an electric field (while heating beyond the glass transition temperature) to partly orient the molecules inside the matrix.[4,7] The results of this poling strategy, however, have not been fully satisfactory, also in view of the limited temporal stability of poled samples. More sophisticated strategies focus on the controlled growth of layers of DA dyes on surfaces *via*, *e.g.*, the Langmuir–Blodgett technique,[8] or the insertion of dyes inside preformed channels of specific materials.[9–12]

Additive behaviour is most often assumed for materials based on DA dyes,[4,7,12] a reasonable hypothesis for very dilute samples where intermolecular interactions are negligible. However, DA dyes are polar and polarizable molecules, and in dense samples, quite impressive cooperative and collective effects are driven by electrostatic intermolecular interactions, as extensively discussed by some of the authors with reference to static NLO responses.[2,13,14] Specifically, depending on the relative orientation and on the nature of the molecules, largely amplified or suppressed responses are predicted, making supramolecular chemistry a powerful tool to engineer the material properties. Important aggregation effects were also recognized in the linear and nonlinear spectral properties of dimers of DA dyes in controlled geometry.[15]

Here, we address a recent experimental work where molecules of 4-dimethylamino-4′-nitrostilbene (DANS), a well-known and widely used DA dye, were encapsulated inside single-wall carbon nanotubes (CNTs) to form DANS@CNT suspensions.[12]

[a] *Department of Chemistry, Life Science and Environmental Sustainability, Parma University, 43124 Parma, Italy. E-mail: anna.painelli@unipr.it*
[b] *New Chemistry Unit and Theoretical Sciences Unit, Jawaharlal Nehru Centre for Advanced Scientific Research, Bangalore-64, India*

† Electronic supplementary information (ESI) available: Experimental procedure, description of the models and validation, preliminary results for aggregates of zwitterionic dyes. See DOI: 10.1039/c7cp04732k

The electrostatic forces acting among the dyes favour their head-to-tail arrangement, leading to linear polar structures whose first hyperpolarizability was addressed by measuring the frequency-resolved Hyper-Rayleigh Scattering (HRS) response. The observed amplification of the β-response was ascribed to the presence of well-ordered chains of dyes containing up to 69 molecules. This large number of aligned molecules was, however, estimated in the hypothesis of additive behaviour (*i.e.*, assuming non-interacting molecules), an assumption that is difficult to reconcile with the observation of a large red-shift (>100 nm) of the linear absorption spectrum of DANS when going from a non-polar solvent (similar to the CNT environment) to the DANS@CNT suspension. This simple observation points to large intermolecular interactions that are expected to heavily affect the β-response of the material.

Here, we present a comprehensive analysis of the optical spectra of DANS in different environments, leading to the conclusion that, if collective and cooperative effects are properly accounted for, the estimated number of aligned molecules needed to reproduce the experimental results for DANS@CNT is reduced by one order of magnitude with respect to the estimate based on the hypothesis of additive behaviour. In the process, we also quantitatively address some experimental features left unexplained in the original paper, giving further support to the proposed interpretation.

Bottom-up modelling of DANS@CNT

The essential-state model for solvated DANS

Fig. 1a collects the linear absorption and fluorescence spectra measured for DANS in different solvents (Experimental details in ESI†), in agreement with literature data.[16] The red-shift of the spectra with increasing solvent polarity, with more important effects in fluorescence than in absorption, is typical of dyes with a weakly polar ground state, whose polarity increases upon excitation.[3] The complex evolution of the optical spectra of DA dyes, including the bandshape evolution, is well captured by

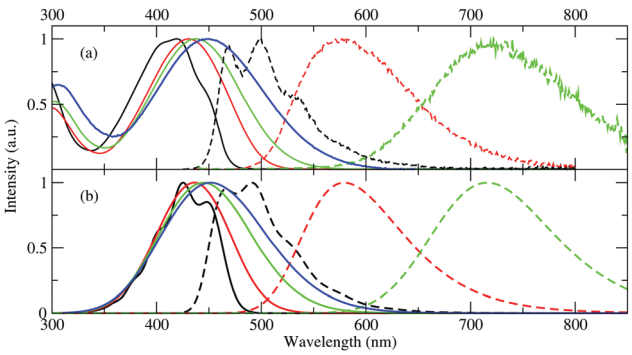

Fig. 1 (a) Normalized absorption and fluorescence spectra (continuous and dashed lines, respectively) of DANS in cyclohexane (black), toluene (red), chloroform (green) and DMSO (blue). (b) ESM simulated spectra, obtained with the molecular model parameters in Table 1 and varying ε_{or} = 0.05, 0.40, 0.90, 1.20 eV to simulate the increasing solvent polarity from cyclohexane to DMSO.

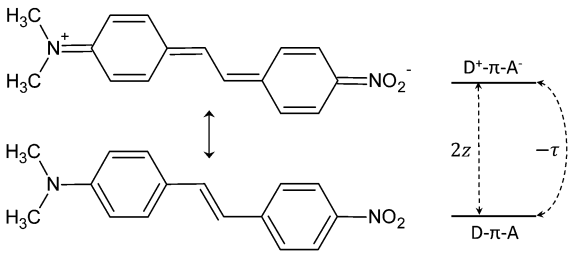

Fig. 2 The two resonating structures of DANS and the corresponding basis states for the essential-state model.

essential-state models[17,18] that account for just two electronic basis states, corresponding to the neutral (D–π–A) and zwitterionic (D^+–π–A^-) resonating structures, as illustrated in Fig. 2. The two basis states are separated by an energy gap $2z$ and are mixed by a matrix element $-\tau$ to give a ground state, $D^{\rho+}$–π–$A^{\rho-}$, characterized by a fractional amount of charge transfer, ρ.

The different geometry of the neutral and zwitterionic basis states is accounted for by introducing a single effective vibrational coordinate with harmonic frequency ω_v and relaxation energy ε_v (see ref. 17–19 and ESI† for the complete model). Four model parameters fully describe the coupled electronic and vibrational problem that is diagonalized numerically in a non-adiabatic approach. Relevant eigenstates enter sum-over-states expressions used to calculate linear and nonlinear optical spectra. An additional parameter, γ, is needed for the calculation of the spectra, measuring the intrinsic bandwidth associated with each vibronic line. To account for polar solvation, the solvent is treated as a dielectric continuum whose interaction with the solute is described by a reaction field that enters the Hamiltonian as a classical coordinate.[17] The corresponding relaxation energy, ε_{or}, is an additional empirical parameter that increases with solvent polarity. Spectra are calculated for different values of the reaction field, and solution spectra are finally obtained by summing the spectra obtained for different values of the reaction field, weighting each contribution for the relevant Boltzmann distribution. Along these lines, an internally consistent treatment of inhomogeneous broadening effects in polar solvents is obtained.[17,18]

The two-state model reproduces very well the complex evolution of the spectral properties of DANS with solvent polarity, as shown in Fig. 1b. Calculated spectra are obtained fixing the 5 molecular parameters listed in Table 1 and increasing ε_{or} to mimic the increasing solvent polarity. We underline that the 4 absorption spectra and the 3 fluorescence spectra (the fluorescence signal in DMSO is too weak to be detected, due to the ω^3 dependence of the fluorescence intensity) in Fig. 1b are calculated in terms of just 9 parameters, a quite impressive result, since a blind fit of the 7 experimental bands in Fig. 1a would require a grand-total of 14 parameters (position and width

Table 1 The molecular model parameters for DANS (eV units)

z	τ	ε_v	ω_v	γ
1.32	0.72	0.30	0.17	0.07

of each band), still not accounting for the resolved vibronic bandshape observed in cyclohexane, which is instead quite naturally addressed in our approach.

Even more interestingly, the same model, derived from the analysis of the linear spectra in Fig. 1, can be used to calculate the nonlinear optical spectra. To address absolute intensities, we fix an additional model parameter μ_0, the dipole moment of the zwitterionic basis state, which is set to 31 D in order to reproduce the molar extinction coefficient at the maximum of the absorption band (ε = 28 000 M^{-1} cm^{-1} in $CHCl_3$). Using sum-over-states expressions (see ESI†), we calculate not only the bandshape, but also the absolute intensity of the nonlinear spectra. Fig. 3 shows the 2PA and HRS spectra calculated for ε_{or} = 0.9 eV, as relevant to chloroform solutions. The shape of the 2PA spectrum is practically superimposed onto the linear absorption spectrum, in line with the results in ref. 20, with a maximum value of ~300 GM, which is slightly overestimated with respect to the experimental result (~220 GM). This discrepancy could be reduced by correcting the calculated spectra for local field effects. More important for our aims are the HRS spectra, reported in Fig. 3 as calibrated HRS signal, S_c^{HRS} (corresponding to β_{zzz}^2 if z is chosen as the molecular axis), according to the definition in ref. 12. The agreement with experiment is striking: our model quite naturally explains the red-shift of the HRS spectrum with respect to the linear absorption resonance, as due to inhomogeneous broadening effects. As for the absolute HRS intensity, the calculated result underestimates the experimental data by a factor of ~4.5. As discussed in ref. 21, this discrepancy could be ascribed to a systematic error in the calibration procedure for HRS signals.

Before closing this section, we underline that popular and nominally parameter-free TD-DFT approaches could be used, with a proper choice of the functional and of the basis set, to obtain reliable estimates of the frequencies and oscillator strengths of the linear absorption band in different solvents, as well as of the frequencies of the fluorescence band. However, standard TD-DFT, as implemented, *e.g.*, in the Gaussian package, does not offer any information about bandshapes. To roughly reproduce the evolution of absorption and fluorescence bandshapes with solvent polarity, without accounting for the vibronic structure, 7 adjustable parameters should be introduced, measuring the bandwidth of the 4 absorption and 3 fluorescence bands in Fig. 1. The Dalton package could be adopted to calculate the nonlinear 2PA and HRS spectra but again, the relevant bandwidths (those for the nonlinear spectra also affect the calculated intensity) should be adjusted by hand, leading to 2 additional parameters to reproduce the spectra in Fig. 3. Moreover, since standard TD-DFT does not account for inhomogeneous broadening, it cannot explain the observed red-shift of the HRS band with respect to the linear absorption band.

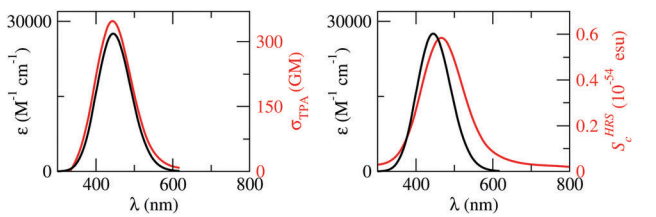

Fig. 3 Calculated nonlinear spectra of DANS in chloroform (red lines). Left: The 2PA spectrum. Right: The calibrated HRS signal (B* convention). In both panels, the black line shows the linear absorption spectrum as the molar extinction coefficient. Spectra are reported against the wavelength associated with the transition frequency, which for 2PA and HRS spectra corresponds to half the photon wavelength.

Building the model for linear aggregates

Having a reliable model for the linear and nonlinear optical properties of DANS in solution, we built a model for the aggregates.[2,13,14] The Hamiltonian of the aggregate was written on the basis obtained as the direct product of the basis states of the monomers. It accounts for intermolecular electrostatic interactions, which affect the energy of the basis states where two or more molecules are in a zwitterionic form (see ESI†). Accounting only for nearest-neighbour interactions, a single interaction term V enters the calculation, measuring the electrostatic interaction energy between two nearby molecules in their zwitterionic form.

The non-adiabatic basis for the coupled vibro-electronic problem increases rapidly with system size, making the problem intractable for large aggregates. As discussed and validated in the ESI,† it is possible to reduce the dimension of the basis accounting only for the in-phase vibration of the molecules in the aggregate. Calculated linear absorption and HRS spectra are shown in Fig. 4 for linear head-to-tail aggregates of increasing size from N = 1 (monomer) up to N = 14. Results are shown for V = −1.35 eV, which, as will be discussed below, is relevant to DANS@CNT, but the approach is more general and applies to aggregates with well delocalized excitations (see ESI†).

As expected for aggregates with attractive intermolecular interactions (negative V), the linear absorption spectrum red-shifts upon increasing the system size,[22] while the bandshape progressively

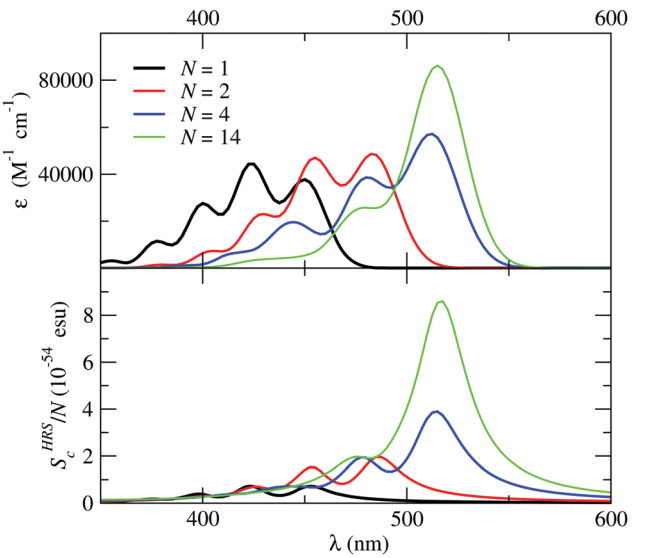

Fig. 4 Results for linear aggregates of N DANS molecules. Top and bottom panels show the linear spectrum (reported as extinction coefficient) and the HRS spectrum (reported as the calibrated HRS signal divided by N) *vs.* the wavelength associated with the transition frequency.

shrinks, pointing to a reduced effective electron-vibration coupling due to exciton delocalization.[23] Indeed the linear and nonlinear spectra calculated for N = 12 and 14 are very similar (see ESI†), suggesting a delocalization length of ~12. The narrowing of the linear absorption band leads to an increase of the maximum molar extinction coefficient, yet, when properly calculated integrating over an energy scale, the area below the linear absorption band stays constant within 5%.

Much more interesting is the behaviour of the HRS spectra. The calibrated S_c^{HRS} signal is an intensive quantity, independent of dye concentration when dealing with solvated dyes.[12] However, in the presence of linear aggregates of non-interacting molecules, S_c^{HRS} is expected to linearly increase with the number of molecules in the aggregate, N.[12] Therefore, in Fig. 4, the calculated results for the linear aggregates are reported as S_c^{HRS}/N, a quantity that is expected to be independent of N for non-interacting molecules. Instead, we observe a fast increase of S_c^{HRS}/N with N, due to intermolecular interactions. This wildly superlinear amplification of the HRS response is in line with early predictions for the static hyperpolarizability (the zero frequency limit of the HRS signal) of aggregates of DA dyes, mainly due to mean-field effects, accounting for the increase of the molecular polarity from solution to the aggregate, and to excitonic and ultraexcitonic effects.[2,13]

We are now in a position to re-analyse the experimental results in ref. 12 properly accounting for intermolecular interactions. The experimental results are reported for two different samples, DANS@oARC and DANS@oHiPco. In both cases, the linear absorption spectrum shows a maximum at $\lambda \sim 500$ nm. According to Fig. 4, the position of the calculated linear absorption spectrum becomes independent of N for $N > 4$, so, unless we expect extremely short aggregates, we can adjust V to reproduce the position of the linear absorption spectrum. Specifically, $V = -1.35$ eV leads to the proper position of the linear absorption band measured for DANS@CNT. The nature of the sample and the shape of experimental spectra suggest the presence of disorder, so we introduce a Gaussian distribution around the average V value. Finally, the number of molecules in the aggregate is fixed to reproduce the experimental amplification of the calibrated S_c^{HRS} signal when going from chloroform solution to the aggregate. The best results in Fig. 5 are obtained for aggregates of 7 dyes with the width of the V distribution set to σ = 0.27 and 0.30 eV to reproduce the experimental bandshapes of the DANS@oARC and DANS@oHiPco samples, respectively.

The agreement between the calculated spectra in Fig. 5 and experimental data in ref. 12 is striking: our model quite naturally reproduces the impressive red-shift of the HRS spectrum, with respect to the linear absorption spectrum, due to inhomogeneous broadening effects, induced by the different dependence of the linear and nonlinear responses upon intermolecular interactions. The experimentally observed amplification of the HRS signal for DANS@CNT is reproduced for a linear aggregate of less than 10 interacting molecules.

As discussed above, the parameter measuring the strength of intermolecular interaction, $V = -1.35$ eV, was fixed to reproduce the position of the linear absorption spectrum of the DANS@CNT sample. The estimate is, however, consistent with simple electrostatic considerations. V, in fact, represents the interaction between two nearby molecules in their zwitterionic state. As a first approximation, V can be calculated as the interaction between two DANS molecules bearing a positive charge on the nitrogen atom of the amino group and a negative charge on the nitrogen atom of the nitro group (*cf.* Fig. 2). According to ref. 12, the intramolecular N–N distance amounts to ~12.27 Å and the intermolecular N–N distance to 4.61 Å, leading to $V \sim -1.9$ eV. This estimate, not accounting for screening effects, represents an upper limit for the interactions, and reasonably agrees with our phenomenological estimate.

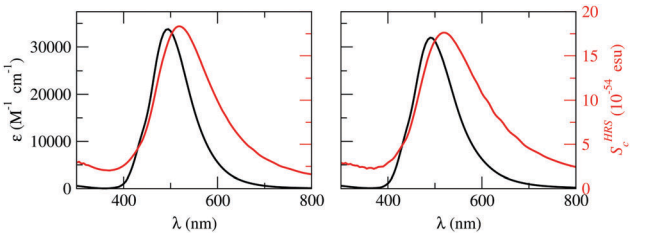

Fig. 5 Linear absorption (black lines) and HRS spectra (red lines) calculated for aggregates of 7 DANS molecules with $V = -1.35$ eV and σ = 0.27 eV (left panel) or σ = 0.30 eV (right panel).

Conclusions

We have presented a comprehensive study of the optical properties of DANS in different environments to build a reliable model for linear aggregates of DANS in CNTs and their unique NLO responses. In a bottom-up modelling approach, we started our analysis demonstrating that a two-state model, parameterized by a handful of molecular parameters, quantitatively reproduces the absorption, florescence, two-photon absorption and HRS spectra of DANS in solution. This model, extensively validated against experimental data, is then extended to aggregates, leading to an internally consistent picture that, naturally accounting for the collective and cooperative amplification of NLO responses due to intermolecular interactions, explains the observed ~30-fold enhancement of the HRS calibrated signal of DANS@CNT *vs.* DANS in solution, in terms of less than 10 aligned molecules. This result sharply contrasts with the estimate of up to 69 aligned molecules that was obtained fully disregarding intermolecular interactions. We underline that in ref. 12, the number of aligned molecules was estimated based on the assumption of non-interacting molecules and on the basis of the HRS signal extrapolated at zero frequency. Since the extrapolation procedure introduces uncontrollable approximations, we prefer to stick to the experimental data in the available spectral window.

The linear absorption band of DANS in solution red-shifts from 420 to 450 nm, when going from cyclohexane to DMSO, and further red-shifts to 500 nm for DANS@CNT. In ref. 12, the red-shift observed in aggregates was ascribed to the strongly polar environment that each dye feels in the aggregate due to surrounding polar DANS molecules. However, a major difference exists between the polar environment experienced

by a dye in solution and in an aggregate. The solvent, in fact, is optically transparent in the spectral region of interest, and the solvent states do not interact (or marginally interact) with the solute states. This is indeed the reason why the dielectric continuum model for the solvent works well. In contrast, in an aggregate, each molecule interacts with nearby equivalent (or almost so) molecules, leading to large cooperative and collective effects stemming from the interaction among (almost) degenerate excited states on nearby molecules.[2,13] The largely red-shifted optical spectra of DANS@CNT confirm, themselves, the large intermolecular interactions and henceforth non-negligible cooperative effects responsible for the non-additive behaviour.

Having discussed the linear aggregates of DANS showing a huge collective and cooperative amplification of the β-response, it is important to mention that for DA dyes with a mostly zwitterionic ground state, *i.e.*, for DA dyes showing an inverse solvatochromism,[3,18] the formation of linear head-to-tail aggregates is detrimental, since a large cooperative suppression of the β response is expected, despite the alignment. The suppression of the static β response for linear aggregates of zwitterionic DA dyes was discussed in ref. 2 and 13. In the ESI†, we show the HRS spectra calculated for linear aggregates of a specific zwitterionic dye.

This work, apart from reanalysing results published in ref. 12, gives an important message to experimentalists. Indeed, we demonstrate that, starting from a DA dye showing normal solvatochromism, it is possible to largely amplify the β-response by organizing just a few molecules in a head-to-tail geometry, without the need to go for very large and experimentally challenging aggregates.

Conflicts of interest

There are no conflicts to declare.

Acknowledgements

The research leading to these results received funding from the People Programme (Marie Curie Actions) of the European Union's Seventh Framework Programme FP7/2007–2013 under REA grant agreement no. 607721 (Nano2Fun). This work was partially supported by Italian MIUR through PRIN2012T9XHH7_002 and by CINECA through IsC43_MMM-CT and IsC50_MMM-time.

Notes and references

1 D.-R. Kanis, M. A. Ratner and T. J. Marks, *Chem. Rev.*, 1994, **94**, 195; S. R. Marder, B. Kippelen, A. K.-Y. Jen and N. Peyghambarian, *Nature*, 1997, **388**, 845; J.-L. Brédas, K. Cornil, F. Meyers and D. Beljonne, in *Handb. Conduct. Polym.*, ed. T. A. Skotheim, R. L. Elsenbaumer and J. R. Reynolds, Marcel Dekker, New York, 2nd edn, 1998, p. 1; M. Albota, J.-L. B. D. Blejonne, J. E. Ehrlich, J.-Y. Fu, A. H. Heikal, S. E. Hess, T. Kogej, M. D. Levin, S. R. Marder, D. McCord-Maughon, J. W. Perry, H. Roeckel, M. Rumi, G. Subramaniam, W. W. Webb, X.-L. Wu and C. Xu, *Science*, 1998, **281**, 1653–1656; M. Rumi, J. E. Ehrlich, A. A. Heikal, J. W. Perry, S. Barlow, Z. Y. Hu, D. McCord-Maughon, T. C. Parker, H. Rockel, S. Thayumanavan, S. R. Marder, D. Beljonne and J. L. Bredas, *J. Am. Chem. Soc.*, 2000, **122**, 9500–9510; M. Barzoukas and M. Blanchard-Desce, *J. Chem. Phys.*, 2000, **113**, 3951–3959; K. D. Belfield, A. R. Morales, B. S. Kang, J. M. Hales, D. J. Hagan, E. W. Van Stryland, V. M. Chapela and J. Percino, *Chem. Mater.*, 2004, **16**, 4634–4641.

2 F. Terenziani, G. D'Avino and A. Painelli, *ChemPhysChem*, 2007, **8**, 2433, and references therein.

3 C. Reichardt, *Chem. Rev.*, 1994, **94**, 2319–2358; G. Hübener, A. Lambacher and P. Fromherz, *J. Phys. Chem. B*, 2003, **107**, 7896; B. Kuhn and P. Fromherz, *J. Phys. Chem. B*, 2003, **107**, 7903.

4 L. R. Dalton, *J. Phys.: Condens. Matter*, 2003, **15**, R897; and references thereinS. R. Marder, L. T. Cheng, B. G. Tiemann, A. C. Friedli, M. Blanchard-Desce, J. W. Perry and J. Skindhoej, *Science*, 1994, **263**, 511; T. Verbiest, S. Houbrechts, M. Kauranen, K. Clays and A. Persoons, *J. Mater. Chem.*, 1997, **7**, 2175; E. D. Rekai, J.-B. Baudin, L. Jullien, I. Ledoux, J. Zyss and M. Blanchard-Desce, *Chem. – Eur. J.*, 2001, **7**, 4395.

5 X. Liu, Z. Yang, D. Wang and H. Cao, *Crystals*, 2016, **6**, 158.

6 D. S. Chemla and J. Zyss, *Nonlinear optical properties of organic molecules and crystals*, Academic Press, Orlando, 1987; J. Zyss, *J. Chem. Phys.*, 1993, **98**, 6583; C. Fave, M. Hissler, K. Senechal, I. Ledoux, J. Zyss and R. Reau, *Chem. Commun.*, 2002, 1674.

7 L. R. Dalton, P. A. Sullivan and D. H. Bale, Electric field poled organic electro-optic materials: state of the art and future prospects, *Chem. Rev.*, 2009, **110**, 25–55; W. Jin, P. V. Johnston, D. L. Elder, K. T. Manner, K. E. Garrett, W. Kaminsky, R. Xu, B. H. Robinson and L. R. Dalton, *J. Mater. Chem. C*, 2016, **4**, 3119.

8 G. J. Ashwell, P. D. Jackson, D. Lochun, P. A. Thompson, W. A. Crossland, G. S. Bahra, C. R. Brown and C. Jasper, *Proceedings: Mathematical and Physical Sciences*, 1994, **445**(1924), 385; G. J. Ashwell, P. D. Jackson, G. Jefferies, I. R. Gentle and C. H. L. Kennard, *J. Mater. Chem.*, 1996, **6**, 137.

9 T. C. T. Pham, H. S. Kim and K. B. Yoon, *Angew. Chem., Int. Ed.*, 2013, **52**, 5539; T. Song, J. Yu, Y. Cui, Y. Yanga and G. Qian, *Dalton Trans.*, 2016, **45**, 4218.

10 K. Komorowska, S. Brasselet, G. Dutier, I. Ledoux, J. Zyss, L. Poulsen, M. Jazdzyk, H.-J. Egelhaaf, J. Gierschner and M. Hanack, *Chem. Phys.*, 2005, **318**, 12; J. Tsuwi, R. Berger, G. Labat, G. Couderc, N.-R. Behrnd, P. Ottiger, F. Cucinotta, K. Schürmann, M. Bertoni, L. Viani, J. Gierschner, J. Cornil, A. Prodi-Schwab, L. De Cola, M. Wübbenhorst and J. Hulliger, *J. Phys. Chem. A*, 2010, **114**, 6956.

11 M. A. Loi, J. Gao, F. Cordella, P. Blondeau, E. Menna, B. Bártová, C. Hébert, S. Lazar, G. A. Botton, M. Milko and C. Ambrosch-Draxl, *Adv. Mater.*, 2010, **22**, 1635; J. Gao, P. Blondeau, P. Salice, E. Menna, B. Bártová, C. Hébert, J. Leschner, U. Kaiser, M. Milko, C. Ambrosch-Draxl and M. A. Loi, *Small*, 2011, **7**, 1807.

12 S. Cambré, J. Campo, C. Beirnaert, C. Verlackt, P. Cool and W. Wenseleers, *Nat. Nanotechnol.*, 2015, **10**, 248.
13 F. Terenziani and A. Painelli, *Phys. Rev. B: Condens. Matter Mater. Phys.*, 2003, **68**, 165405; A. Painelli and F. Terenziani, *J. Am. Chem. Soc.*, 2003, **125**, 5624; A. Painelli, F. Terenziani and Z. G. Soos, *Theor. Chem. Acc.*, 2007, **117**, 915; A. Datta, F. Terenziani and A. Painelli, *ChemPhysChem*, 2006, **7**, 2168.
14 F. Terenziani and A. Painelli, *J. Lumin.*, 2005, **112**, 474; A. Painelli, F. Terenziani and Z. G. Soos, *Theor. Chem. Acc.*, 2007, **117**, 915.
15 A. Painelli, F. Terenziani, L. Angiolini, T. Benelli and L. Giorgini, *Chem. – Eur. J.*, 2005, **11**, 6053; L. Grisanti, F. Terenziani, C. Sissa, M. Cavazzini, F. Rizzo, S. Orlandi and A. Painelli, *J. Phys. Chem. B*, 2011, **115**, 11420; F. Terenziani, M. Morone, S. Gmouh and M. Blanchard-Desce, *ChemPhysChem*, 2006, **7**, 685; F. Terenziani, O. Mongin, C. Katan, B. K. G. Bhatthula and M. Blanchard-Desce, *Chem. – Eur. J.*, 2006, **12**, 3089; F. Terenziani, S. Ghosh, A.-C. Robin, P. K. Das and M. Blanchard-Desce, *J. Phys. Chem. B*, 2008, **112**, 11498.
16 C.-C. Chiu, W.-C. Chen and P.-Y. Cheng, *J. Photochem. Photobiol., A*, 2015, **310**, 26.
17 A. Painelli and F. Terenziani, *J. Phys. Chem. A*, 2000, **104**, 11041; B. Boldrini, E. Cavalli, A. Painelli and F. Terenziani, *J. Phys. Chem. A*, 2002, **106**, 6286–6294.
18 F. Terenziani, A. Painelli, A. Girlando and R. M. Metzger, *J. Phys. Chem. B*, 2004, **108**, 10743; A. Girlando, C. Sissa, F. Terenziani, A. Painelli, A. Chwialkowska and G. J. Ashwell, *ChemPhysChem*, 2007, **8**, 2195.
19 F. Todescato, I. Fortunati, S. Carlotto, C. Ferrante, L. Grisanti, C. Sissa, A. Painelli, A. Colombo, C. Dragonetti and D. Roberto, *Phys. Chem. Chem. Phys.*, 2011, **13**, 11099; L. Grisanti, G. D'Avino, A. Painelli, J. Guasch, I. Ratera and J. Veciana, *J. Phys. Chem. B*, 2009, **113**, 4718.
20 G. Wicks, A. Rebane and M. Drobizhev, *Proc. SPIE*, 2014, **8983**, 89830.
21 J. Campo, A. Painelli, F. Terenziani, T. Van Regemorter, D. Beljonne, E. Goovaerts and W. Wenseleers, *J. Am. Chem. Soc.*, 2010, **132**, 16467.
22 J. Knoester, in *Organic Nanostructures: Science and Applications, Proceedings of the International School of Physics Enrico Fermi, CXLIX Course*, ed. M. Agranovich and G. C. La Rocca, IOS Press, Amsterdam, 2002, and references therein.
23 F. C. Spano, *Annu. Rev. Phys. Chem.*, 2006, **57**, 217.

